The Charge Form Factor of the Neutron at Low Momentum Transfer from the $^2\vec{\mathrm{H}}(\vec{\mathrm{e}},\mathrm{e}'\mathrm{n})\mathrm{p}$ Reaction

E. Geis,[1,*] V. Ziskin,[2,*] T. Akdogan,[2] H. Arenhövel,[3] R. Alarcon,[1] W. Bertozzi,[2] E. Booth,[4] T. Botto,[2] J. Calarco,[5] B. Clasie,[2] C.B. Crawford,[2] A. DeGrush,[2] T.W. Donnelly,[2] K. Dow,[2] M. Farkhondeh,[2] R. Fatemi,[2] O. Filoti,[5] W. Franklin,[2] H. Gao,[6] S. Gilad,[2] D. Hasell,[2] P. Karpius,[5] M. Kohl,[2] H. Kolster,[2] T. Lee,[5] A. Maschinot,[2] J. Matthews,[2] K. McIlhany,[7] N. Meitanis,[2] R.G. Milner,[2] J. Rapaport,[8] R.P. Redwine,[2] J. Seely,[2] A. Shinozaki,[2] S. Širca,[2] A. Sindile,[5] E. Six,[1] T. Smith,[9] M. Steadman,[2] B. Tonguc,[1] C. Tschalaer,[2] E. Tsentalovich,[2] W. Turchinetz,[2] Y. Xiao,[2] W. Xu,[6] C. Zhang,[2] Z. Zhou,[2] and T. Zwart[2]

(The BLAST Collaboration)

[1] *Arizona State University, Tempe, AZ 85287*
[2] *Laboratory for Nuclear Science and Bates Linear Accelerator Center, Massachusetts Institute of Technology, Cambridge, MA 02139*
[3] *Institut für Kernphysik, Universität Mainz, D-55099 Mainz, Germany*
[4] *Boston University, Boston, MA 02215*
[5] *University of New Hampshire, Durham, NH 03824*
[6] *Triangle Universities Nuclear Laboratory and Duke University, Durham, NC 27708-0305*
[7] *United States Naval Academy, Annapolis, MD 21402*
[8] *Ohio University, Athens, OH 45701*
[9] *Dartmouth College, Hanover, NH 03755*

(Dated: January 11, 2008)

We report new measurements of the neutron charge form factor at low momentum transfer using quasielastic electrodisintegration of the deuteron. Longitudinally polarized electrons at an energy of 850 MeV stored in the South Hall Ring (SHR) of the MIT-Bates Linear Accelerator Center were scattered from an isotopically pure, highly polarized deuterium gas target internal to the storage ring. The scattered electrons and coincident neutrons were measured by the Bates Large Acceptance Spectrometer Toroid (BLAST) detector. The neutron form factor ratio G_E^n/G_M^n was extracted from the beam-target vector asymmetry A_{ed}^V at four-momentum transfers $Q^2 = 0.14$, 0.20, 0.29 and 0.42 $(\mathrm{GeV/c})^2$.

PACS numbers: 13.40.-f, 13.40.Gp, 13.88.+e, 14.20.Dh, 25.30.Bf

The uncharged neutron is composed of charged constituents, whose net distribution is described by the charge (or electric) form factor G_E^n. Differences in the up and down quark distributions in the nucleon produce a nonuniform distribution of the net neutron charge. The neutron electric form factor G_E^n exhibits a maximum in the region of $Q^2 \approx 0.1 - 0.5$ $(\mathrm{GeV/c})^2$; when Fourier transformed this corresponds to a positively charged core at small distances and a concentration of negative charge at intermediate to large distances of ≈ 1 fm, commonly associated with a meson cloud surrounding the nucleon. Models which emphasize the role of the meson cloud have been successful in explaining important aspects of nucleon structure [1, 2, 3, 4]. Precise knowledge of G_E^n is essential for the description of electromagnetic structure of nuclei, and for the interpretation of parity violating electron scattering experiments to determine the strangeness content in the nucleon. Further, it is anticipated that exact *ab initio* QCD calculations of G_E^n using lattice techniques will eventually be possible [5].

In the absence of a free neutron target feasible for scattering experiments determinations of G_E^n at finite Q^2 are typically carried out using quasielastic electron scattering from the neutron bound in deuterium or ^{3}He targets. Despite the small value of G_E^n compared to the neutron magnetic form factor G_M^n, it can be obtained with high precision from double polarization observables based on the interference of G_E^n with G_M^n. With the availability of high duty-factor polarized electron beams over the last decade, experiments have employed recoil polarimeters [6], and targets of polarized ^{2}H [7] and ^{3}He [8] to perform precision measurements of G_E^n using polarization techniques with inherently small systematic uncertainties. The slope of $G_E^n(Q^2)$ at $Q^2 = 0$ which defines the neutron square radius is precisely determined by the scattering of thermal neutrons from atomic electrons [9].

This paper reports on new measurements of G_E^n/G_M^n at low Q^2 in the vicinity of the maximum of G_E^n using a longitudinally polarized electron beam incident on a vector-polarized ^{2}H target internal to the South Hall Ring at the MIT-Bates Linear Accelerator Center. The BLAST detector was used to detect quasielastically scattered electrons in coincidence with recoil neutrons over a range of Q^2 between 0.10 and 0.55 $(\mathrm{GeV/c})^2$.

The differential cross section for the $^2\mathrm{H}(\mathrm{e},\mathrm{e}'\mathrm{n})\mathrm{p}$ reaction with polarized beam and target can be written as [10, 11, 12]

$$\begin{aligned} \frac{d^3\sigma}{d\Omega_e d\Omega_{pq} d\omega} &= \sigma_{unp}(1 + \Sigma + P_e\Delta) \\ \Sigma &= \sqrt{\frac{3}{2}} P_z A_d^V + \sqrt{\frac{1}{2}} P_{zz} A_d^T \\ \Delta &= A_e + \sqrt{\frac{3}{2}} P_z A_{ed}^V + \sqrt{\frac{1}{2}} P_{zz} A_{ed}^T, \end{aligned} \tag{1}$$

where σ_{unp} is the unpolarized differential cross section, $P_z = n_+ - n_-$ and $P_{zz} = n_+ + n_- - 2n_0$ are the vector and tensor polarizations of the deuteron target defined by the relative populations n_m of the three deuteron magnetic substates $m = +1, 0, -1$, respectively, and P_e is the longitudinal polarization of the electron beam.

With BLAST, all of the polarization observables A_i in Eq. (1) have been measured for the first time with precision in a single experiment. The beam-target vector polarization observable A^V_{ed} is particularly sensitive to the neutron form factor ratio G^n_E/G^n_M [12]. In the Plane Wave Impulse Approximation (PWIA) and with the deuteron in a pure S-state the asymmetry A^V_{ed} can be written analogously to elastic scattering from the free neutron as

$$\begin{aligned} A^V_{ed} &= \frac{a\, {G^n_M}^2 \cos\theta^* + b\, G^n_E G^n_M \sin\theta^* \cos\phi^*}{c\, {G^n_E}^2 + {G^n_M}^2} \\ &\approx a\cos\theta^* + b\,\frac{G^n_E}{G^n_M}\sin\theta^*\cos\phi^*, \end{aligned} \tag{2}$$

where θ^* and ϕ^* are the target spin orientation angles with respect to the momentum transfer vector and a, b, c are known kinematic factors. This polarization observable exhibits the maximum sensitivity to G^n_E when the momentum transfer vector is perpendicular to the direction of the target polarization, i.e. $\theta^* = 90°$.

However, there are sizable corrections to the asymmetry in Eq. (2), mainly at low Q^2 where they are dominated by final state interactions (FSI); the relative contributions of meson exchange currents (MEC), isobar configurations (IC) and relativistic corrections (RC) become more significant as the momentum transfer increases (see Fig. 1). The final G^n_E extraction must be done from a comparison with theoretical asymmetries that include these effects.

The effects of FSI can be monitored with the other polarization observables in Eq. (1). The asymmetries A_e, A^V_d, and A^T_{ed} all vanish in the Born approximation with parity and time reversal conservation and remain very small (below 1%) even in the presence of FSI, which allows the use of these observables to identify any false asymmetries in the experiment. The effects of FSI gives a sizable contribution to the target tensor asymmetry A^T_d which is insensitive to G^n_E and otherwise close to zero in the quasifree limit. Figure 1 displays a Monte Carlo simulation of the reaction mechanism effects on the asymmetries A^V_{ed} (upper panel) and A^T_d (lower panel) as a function of Q^2 along with the measured values. The calculations use the standard dipole form factor $G_D = (1 + Q^2/0.71)^{-2}$ for G^p_E, G^p_M/μ_p, and G^n_M/μ_n, and $1.91\tau/(1 + 5.6\tau)\, G_D$ for G^n_E [13], where $\mu_p = 2.79$, $\mu_n = -1.91$, and $\tau = Q^2/(4m_n^2)$. Comparing the calculations with the measured tensor asymmetry A^T_d, the value of χ^2/d.o.f. improves from 139.6/4 in PWIA to 6.4/4 under inclusion of FSI, MEC, IC and RC. The excellent agreement of the measured tensor asymmetry A^T_d with the full model validates the calculations of FSI for a reliable extraction of G^n_E from the beam-target vector asymmetry A^V_{ed} at the percent level.

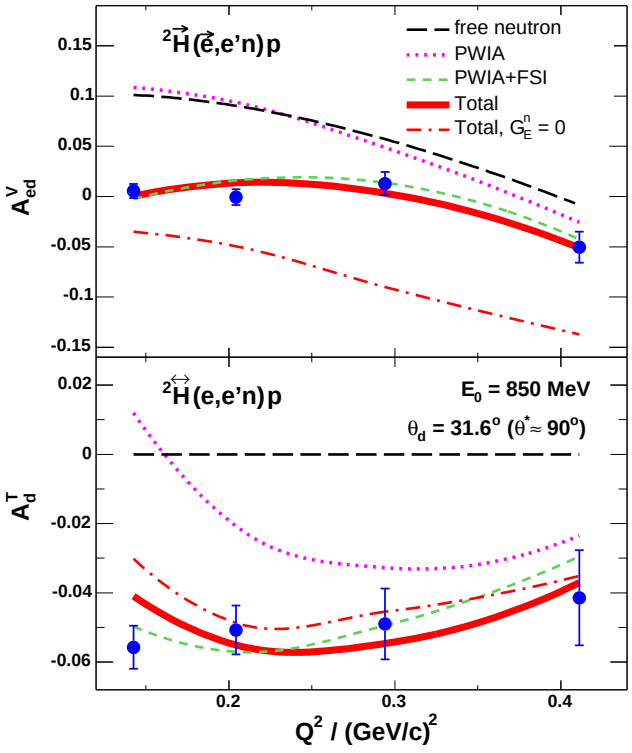

FIG. 1: Measured (solid blue points) and calculated beam-target vector polarization observable A^V_{ed} (upper panel) and tensor asymmetry A^T_d (lower panel) for the ^{2}H(e, e′n)p reaction at 850 MeV, a target orientation of $\theta_d = 31.6°$ into the left sector of BLAST, and with neutrons detected in the right sector. The colored curves are Monte Carlo simulations based on the deuteron electrodisintegration model of Ref. [11] (dotted purple = PWIA, short-dashed green = PWIA+FSI, solid red = PWIA+FSI+MEC+IC+RC) using standard parameterizations for the nucleon form factors (see text). In addition, the corresponding curves for $G^n_E \equiv 0$ (dash-dotted red) and for elastic scattering from the free neutron (dashed black line) are shown. The agreement of the measured tensor asymmetry A^T_d with the full model supports the calculation of FSI for an accurate extraction of G^n_E from A^V_{ed}.

On the other hand, the corrections at low Q^2 to A^V_{ed} measured in the $^2\vec{H}(\vec{e},e'p)n$ reaction in quasifree kinematics are negligible [12] which allows for a precise determination of the product of beam and target polarizations P_eP_z along with the proton form factor ratio G^p_E/G^p_M in this reaction channel [14].

The BLAST experiment was designed to carry out spin-dependent electron scattering from hydrogen [15] and light nuclei. Details on the experimental setup can be found in [16]. The internal target consists of an atomic beam source (ABS) combined with an open-ended storage cell through which the stored electron beam passes continuously [17]. The ABS has been used to sequentially inject polarized monoatomic deuterium gas into the storage cell with nuclear vector ($V+$: m=1; $V-$: m=−1) and tensor ($T-$: m=0) polarization states. In addition, the helicity h of the electron beam was flipped at the source every injection cycle. Linear combinations of the

six charge-normalized yields Y_{hm} define all five polarization observables in Eq. (1). The experimental value of the beam-vector polarization observable A_{ed}^V can be written as

$$A_{ed}^V = \sqrt{\frac{3}{2}} \frac{1}{P_e P_z} \frac{Y_{++} + Y_{--} - Y_{+-} - Y_{-+}}{Y_{tot}}, \qquad (3)$$

where Y_{tot} is the total yield obtained by summing up all six combinations hm. A modest magnetic holding field was applied to define the polarization angle θ_d within the horizontal plane and to minimize the depolarization of target atoms. The non-uniformity of θ_d along the target cell was carefully mapped with movable Hall probes and a compass device. The absolute calibration of the average orientation angle θ_d along with a determination of the tensor polarization P_{zz} was done in situ by comparing the simultaneously measured tensor asymmetries in elastic scattering from tensor-polarized deuterium [18] with those expected at low Q^2 based on a parameterization of world data [19].

The BLAST detector is a toroidal spectrometer with the horizontal sectors instrumented with wire chambers, aerogel Čerenkov counters, thin plastic timing scintillators, and thick plastic scintillator walls for neutron detection. With the target polarization vector pointing into the left sector, the neutron detection efficiency was augmented in the right sector covering the kinematic region most sensitive to the neutron form factor ratio, as indicated by the $\sin\theta^*$ term in Eq. (2) while the detection of neutrons in the left sector was primarily used to independently verify the determination of $P_e P_z$ from the $^2\vec{\mathrm{H}}(\vec{\mathrm{e}},\mathrm{e'p})\mathrm{n}$ reaction.

Figure 2 shows the (e,e'n) yield normalized to the collected beam charge for the measurements with deuterium, hydrogen and empty target. As is evident from the figure, the selection of (e,e'n) events is very clean. A set of cuts applied on the time correlation between the charged and the neutral track, and on kinematic constraints for the electrodisintegration process was employed to identify the quasielastic (e,e'n) events. The background measured with hydrogen (empty) target is less than 4% (3%) of the normalized yield obtained with deuterium. The main sources of the background are quasielastic and inelastic beam halo scattering off the aluminum target cell walls, as well as contributions of the ^{2}H(e,e'n) reaction from above pion production threshold which are suppressed by cuts in the invariant and missing mass spectra.

The small difference in the observed (e,e'n) rate between the empty and hydrogen target in Fig. 2 indicates a negligible number of proton tracks misidentified as neutrons, due to the highly efficient charged particle veto provided by the thin scintillator bars in front of the neutron detectors along with the large-volume drift chambers with 18 active layers, unique to the BLAST detector. Subsequently, the measured raw asymmetry in Eq. (3) has been corrected by up to $\approx 4\%$ for diluting (e,e'n) background events from the aluminum cell walls measured with hydrogen gas in the storage cell.

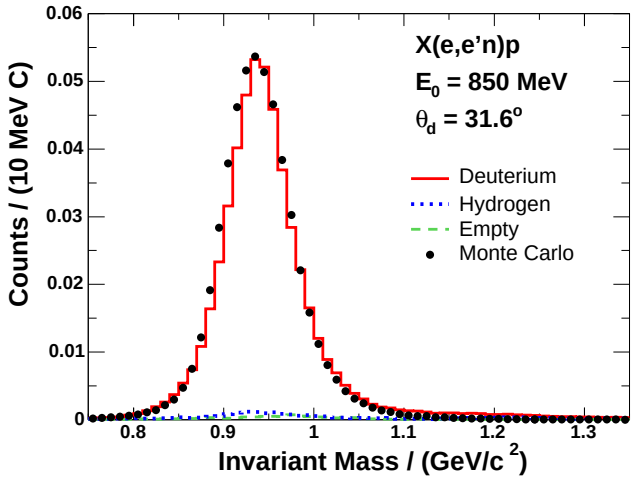

FIG. 2: Measured yields of (e,e'n) events normalized to the accumulated beam charge for deuterium (solid red line), hydrogen (dotted blue line) and empty target (dashed green line), as a function of the invariant mass, shown for the dataset at $\theta_d = 31.6^\circ$. The Monte Carlo data (black circles) have been normalized to the measured yield from deuterium. The peak corresponds to quasielastic scattering. The background measured with hydrogen (empty) target is less than 4% (3%) of the yield obtained with deuterium target.

The corrected asymmetries were compared to the results of Monte Carlo simulations based on the deuteron electrodisintegration model [11], for which events were generated according to the unpolarized cross section and additionally weighted event-by-event with the spin-dependent terms in Eq. (1). The acceptance-averaged asymmetry A_{ed}^V was simulated for different values of G_E^n/G_M^n and compared to the experimental values. In order to extract the best value of the form factor ratio for each Q^2 bin a χ^2 minimization was performed independently with respect to the missing momentum of the reaction and the angle of the neutron in the hadronic center-of-mass system. Both extractions produced consistent results.

The data reported here were acquired in two separate runs in 2004 and 2005, corresponding to a target polarization angle of $31.64^\circ \pm 0.35^\circ(\mathrm{stat}) \pm 0.24^\circ(\mathrm{sys})$ and $46.32^\circ \pm 0.42^\circ(\mathrm{stat}) \pm 0.16^\circ(\mathrm{sys})$, respectively. With a total accumulated beam charge of 451 kC (503 kC) in the first (second) dataset, final samples of 268,914 (205,252) coincident electron-neutron events were collected. The average product of beam and target polarization determined from the $^2\vec{\mathrm{H}}(\vec{\mathrm{e}},\mathrm{e'p})$ reaction was $P_e P_z = 0.5796 \pm 0.0034(\mathrm{stat}) \pm 0.0034(\mathrm{sys})$ in the first and $0.5149 \pm 0.0043(\mathrm{stat}) \pm 0.0054(\mathrm{sys})$ in the second dataset. In comparison, the polarization product determined from $^2\vec{\mathrm{H}}(\vec{\mathrm{e}},\mathrm{e'n})\mathrm{p}$ with neutrons detected in the left sector of BLAST corresponding to $\theta^* \approx 0^\circ$, was found to be $0.587 \pm 0.019(\mathrm{stat})$ for the first and $0.481 \pm 0.026(\mathrm{stat})$ for the second dataset, consistent with the above (e,e'p) results but less precise. The two datasets were treated as separate experiments producing two consistent results

for the form factor ratio, which were combined for a final result. The data were divided into four Q^2 bins selected for the determination of G_E^n/G_M^n with a comparable statistical significance. The results are compiled in Table I.

$Q^2/(\mathrm{GeV/c})^2$	$\langle Q^2\rangle/(\mathrm{GeV/c})^2$	$\mu_n G_E^n/G_M^n$
0.10−0.17	0.142	$0.0505 \pm 0.0072 \pm 0.0030$
0.17−0.25	0.203	$0.0695 \pm 0.0084 \pm 0.0037$
0.25−0.35	0.291	$0.1024 \pm 0.0127 \pm 0.0042$
0.35−0.55	0.415	$0.1172 \pm 0.0182 \pm 0.0046$

TABLE I: Results for the extracted neutron form factor ratio $\mu_n G_E^n/G_M^n$ ($\mu_n = G_M^n(0) = -1.91$) with statistical and systematic errors, respectively.

The systematic error of G_E^n/G_M^n is dominated by the uncertainty of the target spin angle θ_d. Other systematic uncertainties include that of the beam-target polarization product $P_e P_z$, the accuracy of kinematic reconstruction, as well as the dependency on software cuts. The systematic uncertainties were evaluated individually for each Q^2 bin and dataset by combining the errors from each source taking covariances into account; the correlated and uncorrelated categories of the two measurements were then combined for a resulting systematic error of each bin. False asymmetries were studied with the observables A_d^V and A_{ed}^T at the percent level and found to be consistent with zero. Radiative corrections to the asymmetries calculated in a PWBA formalism using the code MASCARAD [20] are <1% and therefore also neglected. The uncertainties of the reaction mechanism and FSI corrections are not included in the total systematic error.

The world's data on G_E^n from double polarization experiments [6, 7, 8] are displayed in Fig. 3 along with the results of this work. All of the polarization data were experimentally determined as electric to magnetic form factor ratios. We used parameterization [21] for G_M^n which is in good agreement with recent measurements [22], to determine G_E^n from BLAST and to adjust the previously published values. The data from a variety of experiments are consistent and remove the large model uncertainty of previous G_E^n extractions from elastic electron-deuteron scattering [23]. The new distribution is also in agreement with G_E^n extracted from the deuteron quadrupole form factor [24].

The measured distribution of G_E^n can be parameterized as a function of Q^2 based on the sum of two dipoles $\sum_i a_i/(1+Q^2/b_i)^2$ $(i = 1,2)$ which is shown as the BLAST fit in Fig. 3 (blue line) with a one-sigma error band. With $G_E^n(0) = 0$ and the slope at $Q^2 = 0$ constrained by $\langle r_n^2\rangle = (-0.1148 \pm 0.0035)$ fm^2 [9] one parameter is fixed, resulting in $a_1 = -a_2 = 0.095 \pm 0.018$, $b_1 = 2.77 \pm 0.83$, $b_2 = 0.385 \pm 0.046$ and $\mathrm{cov}(a_1, b_1) = -0.014$, $\mathrm{cov}(a_1, b_2) = 0.0008$, $\mathrm{cov}(b_1, b_2) = -0.036$ with Q^2 in units of $(\mathrm{GeV/c})^2$. The parameterization [25] (purple long-dashed line) is based on the form introduced in [21] with an additional bump structure around $0.2-0.4$ $(\mathrm{GeV/c})^2$. Also shown are the recent result of a dispersion analysis [4] (green solid line), and the prediction of a light-front cloudy bag model with relativistic constituent quarks [3] (red short-dashed line).

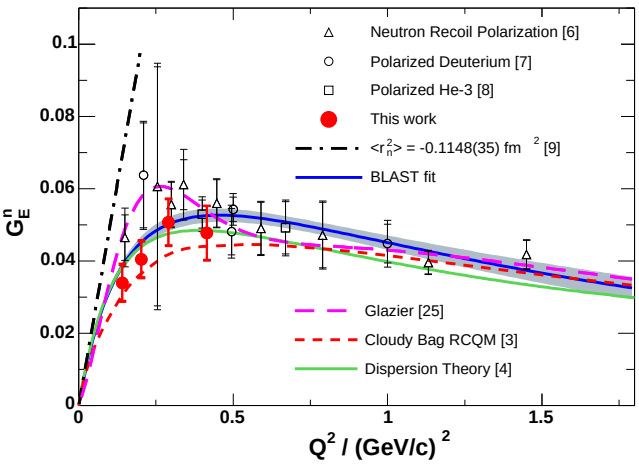

FIG. 3: World data of G_E^n from double polarization experiments. The data correspond to neutron recoil polarization experiments with unpolarized ^{2}H target [6] (open triangles) and experiments with polarized ^{2}H (open circles = Ref. [7], solid red dots = this work) and ^{3}He targets [8] (open squares). The data are shown with statistical (small error bars) and with statistical and systematic errors added quadratically (large error bars). The "BLAST fit" (blue solid line) is a parameterization of the data based on the sum of two dipoles shown with a one-sigma error band. The recent parameterization [25] (purple long-dashed line) is based on the form introduced in [21]. Also shown are the recent result of a dispersion analysis [4] (green solid line), and a light-front cloudy bag model with relativistic constituent quarks [3] (red short-dashed line).

The new data from BLAST do not support a pronounced bump structure at low Q^2 as previously suggested [21, 25]. The BLAST data are in excellent agreement with the dispersion analysis [4] and also agree well with the meson-cloud model [3]. The improved precision of the now available data at low Q^2 provides strong constraints on the theoretical understanding of the nucleon's meson cloud.

We thank the staff of the MIT-Bates Linear Accelerator Center for the deliver of high quality electron beam and for their technical support.

This work has been supported in part by the US Department of Energy and National Science Foundation.

* Reported results are based on the Ph.D. theses of E.G. and V.Z.

[1] Z. Dziembowski *et al.*, Ann. Phys. **258**, 1 (1997).
[2] B. Pasquini and S. Boffi, Nucl. Phys. **A782**, 86 (2007).
[3] G.A. Miller, Phys. Rev. C **66**, 032201 (2002).
[4] M.A. Belushkin, H.-W. Hammer, and U.-G. Meissner, Phys. Rev. C **75**, 035202 (2007).
[5] C. Alexandrou, G. Koutsou, J.W. Negele, and A. Tsapalis, Phys. Rev. D **74**, 034508 (2006).
[6] B. Plaster *et al.*, Phys. Rev. C **73**, 025205 (2006); D.I. Glazier *et al.*, Eur. Phys. J. A **24**, 101 (2005);

R. Madey *et al.*, Phys. Rev. Lett. **91**, 122002 (2003); T. Eden *et al.*, Phys. Rev. C **50**, R1749 (1994).
[7] H. Zhu *et al.*, Phys. Rev. Lett. **87**, 081801 (2001); I. Passchier *et al.*, Phys. Rev. Lett. **82**, 4988 (1999).
[8] J. Golak *et al.*, Phys. Rev. C **63**, 034006 (2001) applying FSI corrections to J. Becker *et al.*, Eur. Phys. J. A **6**, 4988 (1999); J. Bermuth *et al.*, Phys. Lett. **B564**, 199 (2003) superseding D. Rohe *et al.*, Phys. Rev. Lett. **83**, 4257 (1999).
[9] S. Kopecky *et al.*, Phys. Rev. Lett. **74**, 2427 (1995); Phys. Rev. C **56**, 2229 (1997).
[10] T.W. Donnelly and A.S. Raskin, Ann. Phys. **169**, 247 (1986).
[11] H. Arenhövel, W. Leidemann, and E.L. Tomusiak, Eur. Phys. J. A **23**, 147 (2005); Phys. Rev. C **46**, 455 (1992).
[12] H. Arenhövel, W. Leidemann, and E.L. Tomusiak, Z. Phys. A **331**, 123 (1988); Erratum Z. Phys. A **334**, 363 (1989).
[13] S. Galster *et al.*, Nucl. Phys. **B32**, 221 (1971).
[14] A. Maschinot, Ph.D. thesis, Massachusetts Institute of Technology, 2005; A. DeGrush, Ph.D. thesis, Massachusetts Institute of Technology, in preparation; A. DeGrush *et al.*, to be published.
[15] C.B. Crawford *et al.*, Phys. Rev. Lett. **98**, 052301 (2007).
[16] D. Hasell *et al.*, The BLAST Experiment (to be published).
[17] D. Cheever *et al.*, Nucl. Instrum. Methods Phys. Res., Sect. A **556**, 410 (2006); L.D. van Buuren *et al.*, Nucl. Instrum. Methods Phys. Res., Sect. A **474**, 209 (2001).
[18] C. Zhang, Ph.D. thesis, Massachusetts Institute of Technology, 2006; C. Zhang *et al.*, to be published.
[19] D. Abbott *et al.*, Eur. Phys. J. A **7**, 421 (2000).
[20] A. Afanasev, I. Akushevich, and N. Merenkov, Phys. Rev. D **64**, 113009 (2001).
[21] J. Friedrich and Th. Walcher, Eur. Phys. J. A **17**, 607 (2003).
[22] **G_M^n from unpolarized quasielastic scattering:** G. Kubon *et al.*, Phys. Lett. **B524**, 26 (2002); H. Anklin *et al.*, Phys. Lett. **B428**, 248 (1998); H. Anklin *et al.*, Phys. Lett. **B336**, 313 (1994); A. Lung *et al.*, Phys. Rev. Lett. **70**, 718 (1993); S. Rock *et al.*, Phys. Rev. Lett. **49**, 1139 (1982); K.M. Hanson *et al.*, Phys. Rev. D **8**, 753 (1973);
G_M^n from polarized ^{3}He: B. Anderson *et al.*, Phys. Rev. C **75**, 034003 (2007); W. Xu *et al.*, Phys. Rev. C **67**, 012201 (2003); W. Xu *et al.*, Phys. Rev. Lett. **85**, 2900 (2000); H. Gao *et al.*, Phys. Rev. C **50**, R546 (1994).
[23] S. Platchkov *et al.*, Nucl. Phys. **A510**, 740 (1990).
[24] R. Schiavilla and I. Sick, Phys. Rev. C **2364**, 041002R (2001).
[25] D.I. Glazier *et al.*, Eur. Phys. J. A **24**, 101 (2005).